

RELIABLE SINGLE DIODE PATCH ANTENNA WITH DUAL MODE FREQUENCY AND PATTERN RECONFIGURABILITY WITH COMPLIANCE ANALYSIS

Sameer Mansuri¹, Shahid S. Modasiya²

¹Research Scholar, Gujarat Technological University, Ahmedabad, Gujarat, India

²Associate Professor, EC Engineering, V.G.E.C., Chandkheda, Gujarat, India
sameer.mansuri@gecmodasa.ac.in¹, shahid@vgecg.ac.in²

Abstract

This study introduces a compact rectangular patch antenna that achieves frequency reconfiguration using a single PIN diode, enabling two distinct operational modes. The design integrates multiple strategically placed slots within the patch to support a wide range of wireless communication bands. By employing only one diode, the antenna reduces circuit complexity and fabrication cost while ensuring efficient performance. The optimization was carried out through full-wave electromagnetic simulations, with reflection coefficients and radiation patterns serving as primary evaluation metrics. A prototype fabricated on a cost-effective FR4 substrate was tested in an anechoic chamber, showing strong correlation between simulated and measured results, with effective impedance matching. Furthermore, reliability assessments and electromagnetic safety evaluations confirmed compliance with international SAR standards and consistent performance under environmental stress conditions. This work highlights that carefully designed slot integration on FR4 substrates can provide performance levels comparable to those of specialized high-frequency materials, delivering a compact and economical solution for modern communication systems.

Keywords: PIN diode, pattern reconfigurable antenna, frequency reconfigurable antenna, and rectangle patch antenna

I. Introduction

The swift progress in wireless communication requires devices to manage several applications at once. Employing distinct antennas for each purpose is unfeasible due to space and complexity constraints. Reconfigurable antennas provide a solution by flexibly altering their operating frequency, polarization, or radiation properties, thereby streamlining hardware design and reducing the number of components [1]. Their versatility highlights their significance in cutting-edge wireless systems in applications including cognitive radio, satellite connectivity, and medical technology.

A microstrip antenna with dual U-slots achieves a 68% bandwidth (1.98–4 GHz) for radar applications [2]. A textile-based design uses PIN diodes and a T-slot to switch between 1.8–2.4 GHz, ensuring safety for wearables [3]. Another study employs slits and PIN diodes for frequency (4.5–5.8 GHz) and pattern reconfiguration [4]. A slot antenna with two switches supports WLAN/ITU bands (2.4–7.8 GHz) in multiple modes [5]. A U-slotted antenna targets Wi-Fi/Wi-Max across L, S, C, and X bands [6]. Our proposed antenna leverages a single PIN diode and three slots to achieve dual-mode operation (Mode 1: 5 GHz, 7.75 GHz; Mode 2: 3.10 GHz, 5.55 GHz, 7.15 GHz, 7.75 GHz), offering a streamlined, cost-effective solution for modern multi-band communication networks.

Researchers have investigated diverse techniques to advance reconfigurable antenna designs. Slot-based modifications, such as CPW-fed bowtie slots, enable single, dual, or triple-band operation (2.4–3.5 GHz) for WiFi/WiMAX [7]. Microstrip-fed bowtie slots enhance bandwidth with switch integration for impedance matching [8]. Dual-band patch antennas with varactors allow independent frequency tuning and distinct radiation patterns [9]. Rhombus-shaped radiators with PIN diodes offer frequency (5.2–5.8 GHz), pattern, and polarization switching [10]. Tapered slot antennas with T/C

resonators and PIN diodes support wideband or multi-band modes (0.97–3.76 GHz) [11]. Slot antennas with slits and switches achieve frequency (1.82–2.10 GHz) and beam angle reconfiguration [12]. Bended dipole-loop designs steer beams ($\pm 50^\circ$) for wearables [13]. Varactor-based dipoles tune frequencies (1.98–2.76 GHz) for WLAN/LTE [14]. These advancements inform our design, which uses a single PIN diode and three slots to achieve dual-mode operation (3.10–7.75 GHz), simplifying control and enhancing efficiency for multi-band wireless applications compared to complex multi-switch configurations [7–14].

In multi-band wireless systems, reconfigurable antennas are critical for compact designs. Techniques like pentagon slot resonators with PIN diodes enable switching between wideband and multi-band modes [15]. Slot length adjustments using six PIN diodes achieve frequency and pattern reconfiguration in S/C bands (2–6 GHz) [16]. Circular disk antennas with 15 PIN diodes offer multi-mode operation for WiMAX/WLAN [17]. Varactor-based center-shortened patches tune dual-band frequencies [18]. Photo-conductive switches in plug-hole designs reconfigure frequency/pattern (2–4 GHz) [19]. Graphene pads shift CPW-fed monopoles from 5G to 4G bands (1.8–7.8 GHz) [20]. Triangle monopoles with PIN diodes tune 1.64–2.54 GHz [21].

A FR4 substrate measuring 55.2 mm \times 50.8 mm with a dielectric constant of 4.4 is employed in this study to design a reconfigurable rectangular patch antenna. It features a 21 mm \times 15 mm inner patch within a 36 mm \times 25.2 mm inverted U1-shaped outer patch. A single PIN diode and three slots (two at 7.5 mm \times 18 mm) enable frequency reconfiguration for multi-band wireless applications.

The motivation is to provide a cost-effective, compact solution for multi-band systems using affordable materials. Full-wave simulations optimize the slot geometry, achieving Mode 1 (5 GHz, 7.75 GHz) and Mode 2 (3.10 GHz, 5.55 GHz, 7.15 GHz, 7.75 GHz). Performance is validated through anechoic chamber tests, offering engineers a detailed reference for developing reconfigurable antennas with enhanced efficiency.

II. Design Methodology

The design methodology for the proposed reconfigurable patch antenna, employs a systematic framework, leveraging electromagnetic theory, computational simulation, and experimental validation. The evolution of the design stages is illustrated in Figure 1, with the corresponding S_{11} characteristics and frequency bands depicted in Figure 2, providing a comprehensive overview of the antenna's performance across its development phases.

I. Structural Design and Material Selection of the Antenna

The development of the reconfigurable antenna starts by constructing a conventional rectangular microstrip patch on an FR4 substrate with dimensions of 55.2 mm by 50.8 mm. The FR4 material, characterized by a dielectric constant $\epsilon_r = 4.4$, is selected for its affordability and widespread availability in printed circuit board (PCB) fabrication. Despite its higher dielectric losses compared to specialized microwave substrates, FR4 offers a practical trade-off between performance and cost for prototyping and compact device integration.

The initial antenna structure (Antenna 1) consists of an outer patch measuring 36 mm \times 25.2 mm, excited through a 20 mm \times 3 mm inset microstrip feed line designed to achieve impedance matching. This arrangement yields a single resonant frequency at 5.58 GHz, as illustrated in Figure 1. The corresponding simulated S_{11} response in Figure 2 indicates a return loss below 10 dB, confirming good impedance matching and establishing a solid baseline for reconfigurable enhancements.

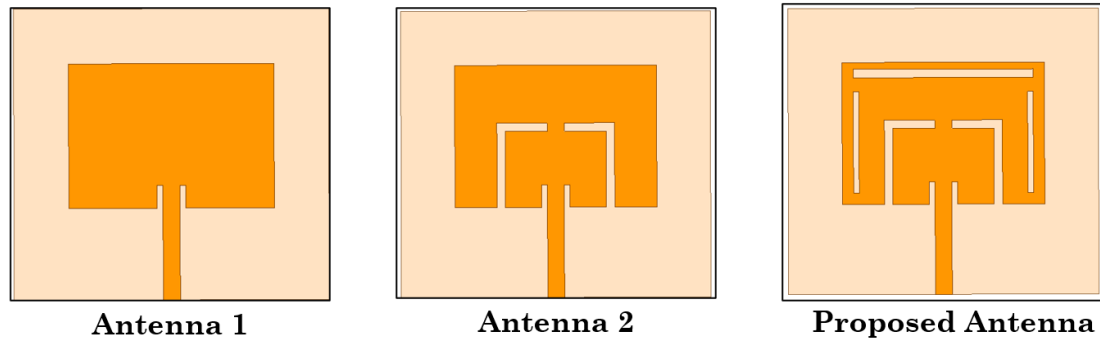


Figure 1. Evolution steps of proposed frequency and pattern reconfigurable antenna.

An inverted U-shaped slot of width 2 mm is incorporated into the outer patch of Antenna 2 to enable frequency reconfigurability, enclosing a 21×15 mm inner patch. A single PIN diode integrated within the slot, controlled by a DC bias, switches between two states: ON, electrically connecting the patches and resonating at 3.88 GHz, and OFF, isolating them and resonating at 2.4 GHz. Simulated S_{11} results in Figure 2 confirm dual-band performance with return losses below -10 dB, demonstrating efficient frequency agility and compact design.

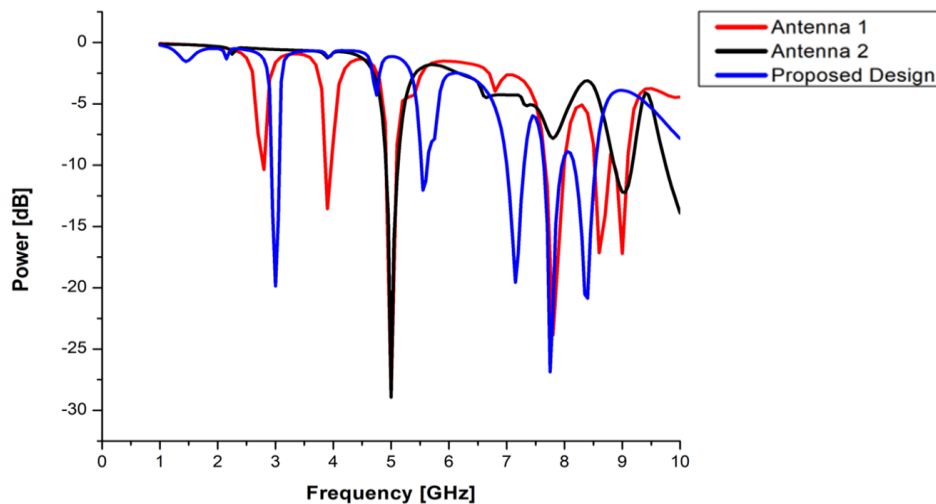


Figure 2. Comparison of simulated S_{11} for the baseline outer patch design (Antenna 1), the reconfigurable dual-band design (Antenna 2), and the proposed multi-band, pattern-reconfigurable patch antenna (Proposed Antenna).

The proposed antenna enhances functionality by adding three slots to the inverted U-shaped structure for multi-band and pattern reconfigurability. Figure 1 shows two vertical slots (7.5 mm \times 18 mm) symmetrically placed and one horizontal slot of the same size at the top. These modifications generate additional current paths, shifting resonant modes and altering field distribution. As illustrated in Figure 2, Mode 1 (PIN diode ON) resonates at 5.00 and 7.75 GHz, while Mode 2 (PIN diode OFF) resonates at 3.10, 5.55, 7.15, and 7.75 GHz. Pattern reconfiguration occurs at 7.15 and 7.75 GHz, demonstrating variation in radiation across modes. Full-wave simulations validate the antenna's compact and reconfigurable design. The structure effectively supports multi-band wireless communication with a single switching element.

Additionally, pattern reconfiguration is observed at 7.15 GHz and 7.75 GHz, indicating variation in radiation characteristics across different modes. These results, obtained through full-wave electromagnetic simulation, confirm the antenna's suitability for multi-band wireless communication systems, offering both compactness and configurability with a single switching component.

II. Full-Wave Electromagnetic Simulation

The developed reconfigurable patch antenna was evaluated using Ansys HFSS full-wave simulations, enabling precise modeling of electromagnetic behavior, including current distribution, resonant frequencies, and radiation characteristics affected by geometry and switching. The simulation process was structured into the following key stages:

I. Model Construction:

The entire antenna geometry including the outer rectangular patch, the inner patch, inverted U-shaped slot, and additional side and top slots were meticulously modelled within HFSS. Fine meshing was applied to critical areas, especially around the slot edges and diode region, to capture high-frequency field variations.

To ensure comprehensive analysis and model validation, Figure 3 shows the fabricated antenna geometry used for both simulation and experimental stages. It provides detailed views of the antenna's top layout (including the slot configuration and feedline) and the bottom copper plane.

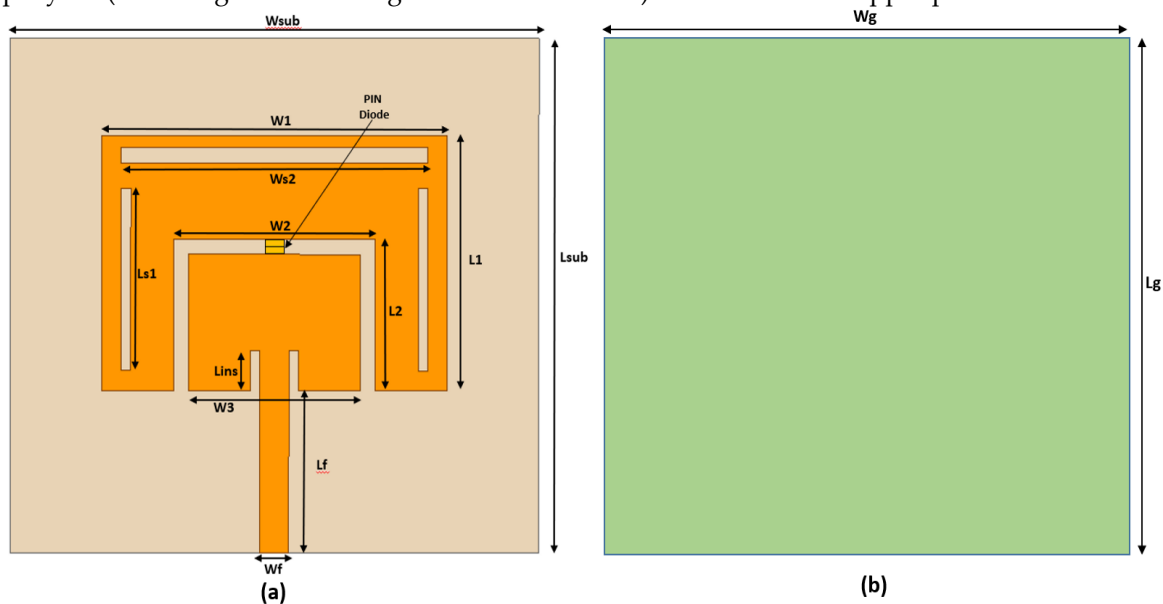


Figure 3. Antenna proposal (a) top view (b) bottom view.

All critical dimensions — such as patch sizes, slot lengths, feed dimensions, and substrate thickness were configured according to the optimized values obtained through parametric analysis (Table 1). The substrate was modelled as FR4 with featuring $\epsilon_r = 4.4$ featuring a 1.6 mm-thick dielectric layer.

II. Boundary Conditions and Excitation

The model used radiation boundaries to emulate free-space conditions and a wave port to excite the antenna through the microstrip feedline. Frequency sweeps and adaptive meshing ensured accurate return loss predictions and convergence of simulation results.

III. PIN Diode Modelling

A Skyworks SMP1345-079LF PIN diode was modeled using equivalent RLC circuits to represent ON and OFF states. In the ON state, low resistance ensures RF continuity between the patches, while the OFF state's high resistance isolates them. These models were embedded as lumped elements across the

U-slot in HFSS. A separately designed bias network with RF chokes and DC-block capacitors ensured DC–RF isolation.

IV. Output Parameters and Analysis

Key output parameters obtained from HFSS include:

- Return Loss (S_{11}): Used to identify resonant frequencies and assess impedance matching in both switching states.
- Electric Field Distribution: To visualize the field intensity and validate active current regions for each resonant mode.
- Surface Current Paths: To study the reconfigurability behavior when switching between modes.
- Gain and Radiation Patterns: To be compared with experimental results.

III. Antenna Design Parameters

To ensure optimal performance and impedance matching across desired bands, key geometrical parameters of the proposed antenna were optimized through parametric analysis using Ansys HFSS. Table 1 presents the finalized dimensions of the antenna’s components, including the patch sizes, slot dimensions, inset feed, and ground plane.

Table 1. Geometrical Parameters and Corresponding Values

Parameter	Value (mm)	Parameter	Value (mm)
W_{sub}	55.2	W_3	18
L_{sub}	50.8	W_g	55.2
W_1	36	L_g	50.8
L_1	25.2	W_f	3
W_2	21	L_f	20
L_2	15	L_{in}	4.6
L_{s1}	18	W_{s2}	32

IV. Simulation Results

The frequency and pattern reconfigurability of developed antenna were evaluated using full-wave simulations in Ansys HFSS with an equivalent RC model of the SMP 1345-079LF PIN diode. The diode operates as a short circuit in the ON state, linking the inner and outer patches, and as an open circuit in the OFF state, isolating them. A biasing network ensures proper DC–RF isolation during operation.

I. Return Loss (S_{11}) Analysis

The antenna’s reflection coefficient (S_{11}) was measured for both switching conditions:

- Mode 0 (Diode OFF): The antenna resonates at 3.10 GHz and 5.55 GHz.
- Mode 1 (Diode ON): Resonant frequencies appear at 5.00 GHz, 7.15 GHz, and 7.75 GHz.

As depicted in Figure 4, the return loss was evaluated through both simulation and physical testing, exhibiting strong agreement and demonstrating effective impedance matching ($S_{11} < -10$ dB) across the operating bands.

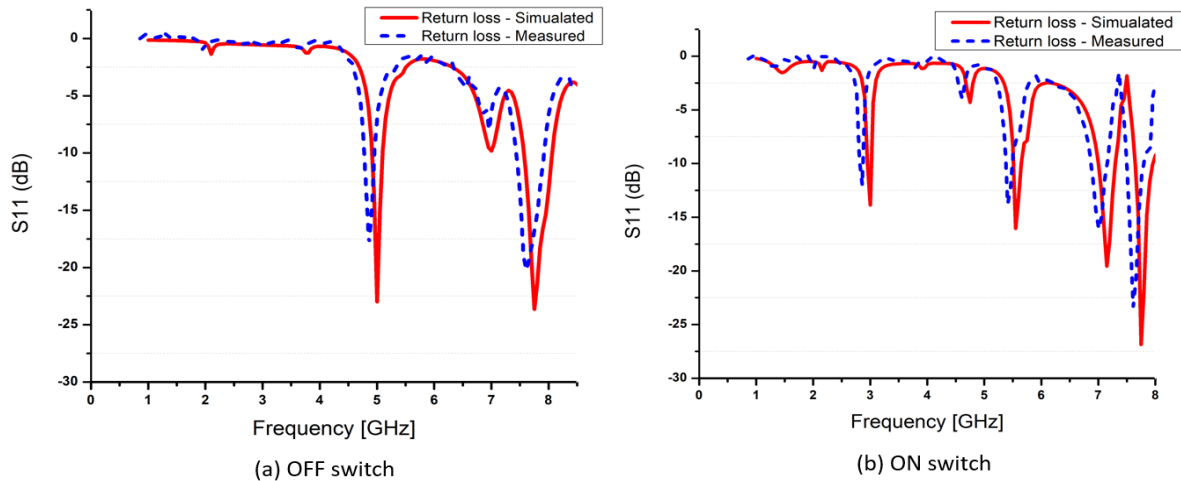


Figure 4. Return loss measurement for proposed antenna in (a) Mode 0 and (b) Mode 1

Performance validation of simulated vs. measured frequency bands is summarized in Table 2.

Table 2. Prototype Evaluation: Correlating Simulated and Experimental Outcomes

PIN diode state	No. of frequency bands	Frequency (GHz)	Return loss (dB) (Simulated)	Return loss (dB) (Measured)
Off	2	5	-23	-17
		7.75	-24	-21
On	4	3.10	-18	-15
		5.55	-16	-13
		7.15	-22	-17
		7.75	-26	-23

II. Electric Field Distribution

Electric field distributions at resonant frequencies reveal distinct behavior in both modes. In the OFF state, strong fields appear along inner patch edges, indicating isolation and longer paths, while in the ON state, continuous flow across patches yields shortened paths and shifted resonance, as shown in Figure 5.

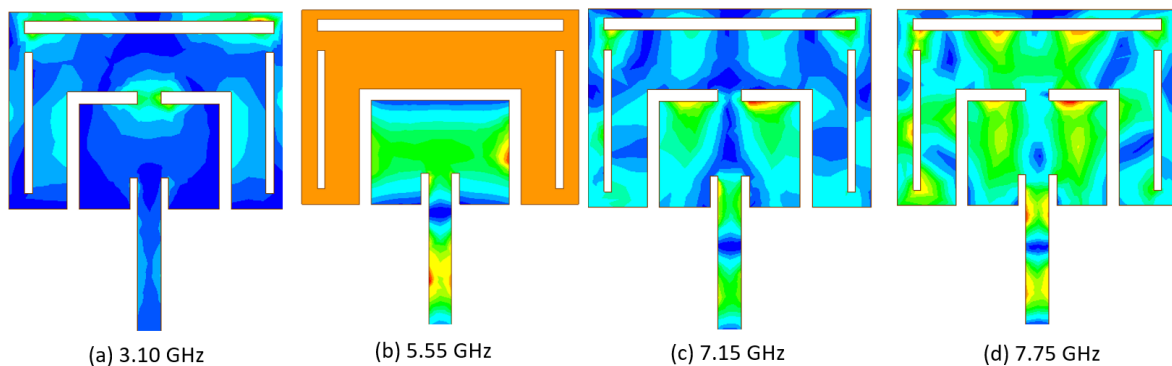


Figure 5. Simulated electric field distribution at various resonant frequencies

III. Radiation Pattern

Simulated and experimental far-field patterns at 3.10, 5.00, 5.55, 7.15, and 7.75 GHz are compared in Figure 6. The results confirm stable directional radiation with favorable front-to-back ratio and consistent patterns across modes.

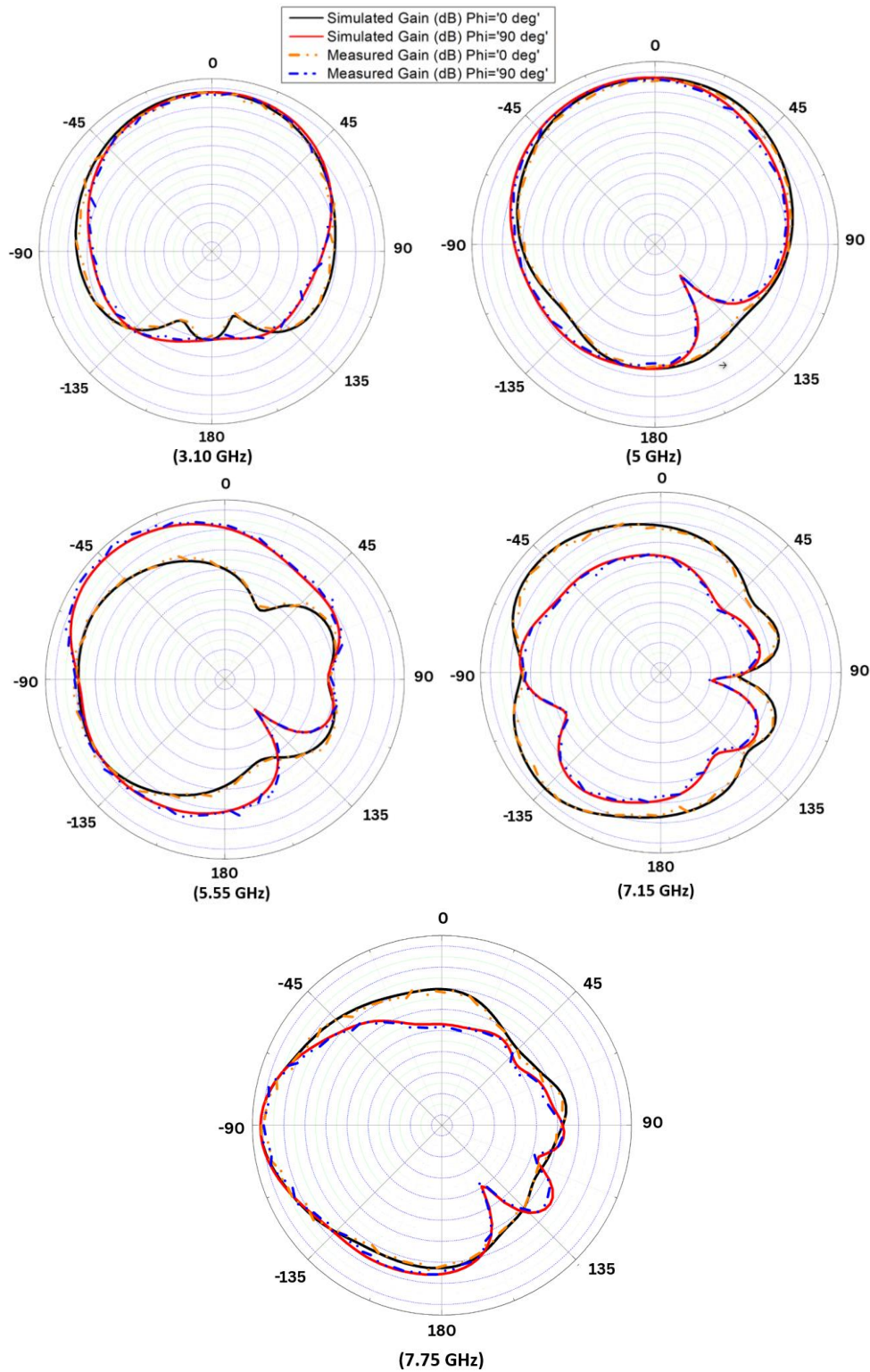


Figure 6. Radiation pattern comparison of proposed antenna between simulated and measured results at different frequencies

III. Results & Discussion

The antenna was prototyped on an FR4 substrate ($\epsilon_r = 4.4$, thickness = 1.6 mm) to evaluate and validate the simulated performance. The antenna geometry, including the outer patch, slots, and biasing circuitry, was accurately replicated on the board using standard PCB fabrication techniques. A single PIN diode was mounted at the designated slot location using surface-mount soldering. The final fabricated design is presented in Figure 7, depicting the antenna from both the top and bottom perspectives. The top side features the radiating patch, slot configurations, and diode placement, while the bottom view highlights the feedline, ground plane, and DC biasing elements.

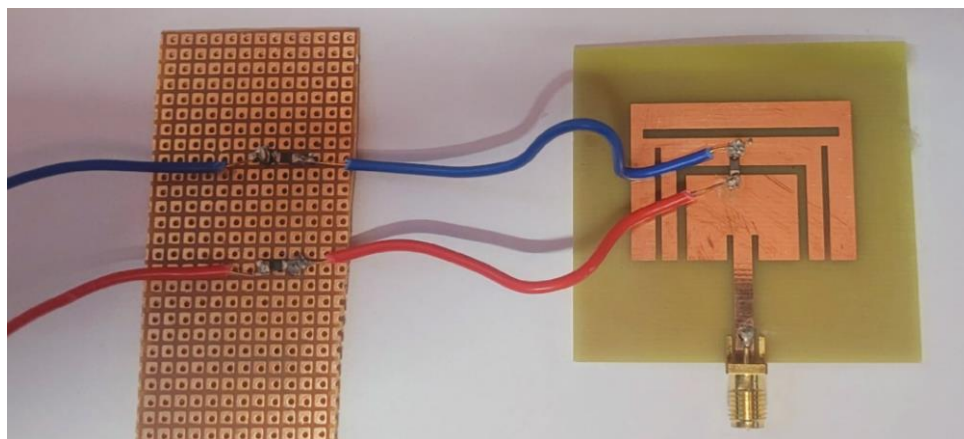


Figure 7. *Fabricated prototype of the proposed antenna*

Experimental validation of the antenna design was conducted in a shielded anechoic chamber, employing a calibrated VNA for accurate measurements. The antenna was connected via an SMA connector, and operational modes were toggled by applying a controlled DC bias across the integrated PIN diode. To ensure effective separation of RF and DC paths, chip inductors and capacitors were used in the biasing circuit, mirroring the simulation configuration. Figure 8 illustrates the measurement setup, with Figure 8(a) showing the VNA connection for return loss testing and Figure 8(b) presenting the chamber arrangement for capturing radiation patterns and gain. The measured return loss remained below -10 dB across all resonant frequencies in both operational modes, indicating strong impedance matching. Gain measurements revealed values ranging from 3.69 dBi to 5.59 dBi, with a peak gain of 5.59 dBi observed at approximately 7.75 GHz.

The close alignment between measured and simulated results validates the robustness of the proposed design methodology and the efficacy of using slot-based reconfiguration in combination with a single PIN diode. This design approach not only enables effective frequency and pattern reconfigurability but also minimizes complexity by reducing the need for multiple switching elements and associated circuitry. The compact size, broad operational bandwidth, and reliable radiation characteristics make the antenna well-suited for modern multi-band wireless communication systems. A comparative analysis with existing reconfigurable patch antennas is presented later in this section to highlight the improvements in key parameters such as gain, bandwidth, frequency agility, and substrate efficiency.

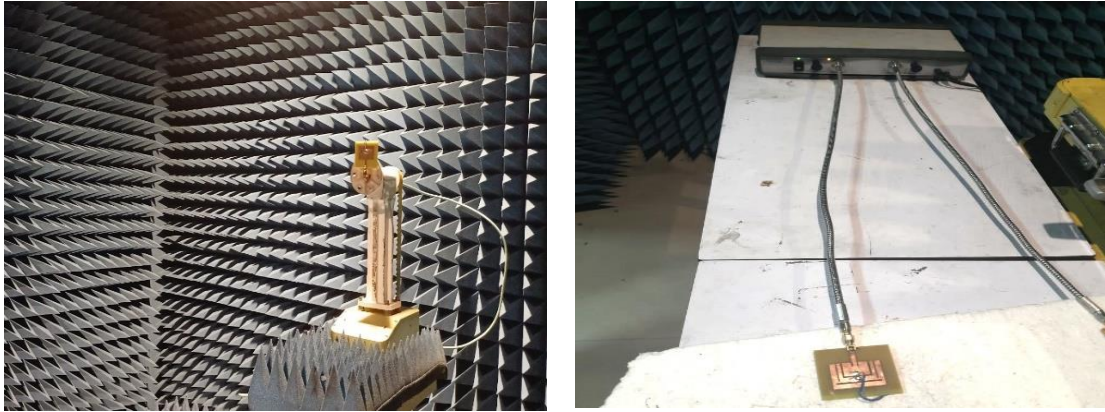


Figure 8. Measurement set of proposed antenna (a) Measurement of the radiation pattern in anechoic chamber
 (b) Measurement of S11

This measurement setup enabled precise characterization of key antenna parameters, including return loss, radiation patterns, and gain in both switching states. By replicating simulation conditions in the prototype, measured data were directly compared with simulations, providing strong validation of the design. The close agreement between results confirms the effectiveness of the slot-based reconfiguration and single PIN diode switching.

The fabricated antenna’s performance aligns well with simulations, with only minor differences caused by fabrication tolerances, soldering inaccuracies, and parasitic losses near the PIN diode. To highlight novelty and competitiveness, a comparative study with recent reconfigurable antennas was conducted. Table 3 summarizes this comparison, covering frequency range, reconfigurability type, number of switches, substrate, and design complexity.

Table 3. Result validation through Comparison of simulation and testing results for proposed antenna prototype

Ref	Size(mm3)	No. of switches	Reconfigurable frequency (GHz)	Pattern reconfigurable	Maximum gain (dBi)
4	50*50*1.6	4	4.5&4.8/5.2&5.8	Yes	3.8
6	61*38*1.5	3	2 to 10(8 bands)	NA	NA
7	80*30*1.6	4	2.4 to 6.5(4 bands)	No	4.5
10	60*50*1.6	3	5.2,5.8	Yes	3
14	30*49*1.61	8	1.98 to 2.76 (Multiband)	No	1.8
17	60*40*1.6	12	2.3 to 5.87 (4 bands)	Yes	12.87
19	60*66*1.6	4	2.96 and 3.26	Yes	3.29
20	50*45*1.52	5	2,3,5 and 5.3	Yes	1.8
21	40*50*0.254	2	1.64 to 2.54 (3 bands)	Yes	NA
Prop.	50.8*55.2*1.6	1	3.10,5,5.55,7.15,7.75	Yes	5.59

The proposed antenna stands out by achieving both frequency and pattern reconfigurability using only a single PIN diode, thereby significantly reducing circuit complexity, minimizing potential RF distortion, and simplifying the DC biasing network. Additionally, the careful placement of biasing components away from the active radiating structure preserves radiation efficiency. These advantages demonstrate that the proposed antenna offers a compact, low-cost, and high-performance solution suitable for modern multi-band wireless communication systems.

IV. Reliability and Compliance

To ensure the proposed frequency and pattern-reconfigurable antenna is suitable for real-world deployment, special attention was given to structural reliability and robustness during the design and fabrication stages. The antenna was implemented on a 1.6 mm thick FR4 substrate with copper metallization materials known for their wide availability and acceptable mechanical stability. The design accounts for practical tolerances during etching and soldering, and the layout avoids abrupt current transitions that could lead to localized heating or stress during continuous operation.

In terms of electrical reliability, the single PIN diode switching mechanism was carefully integrated to minimize circuit complexity and reduce the chances of failure due to multiple biasing elements. The diode placement ensures consistent switching performance, and the use of RF choke components helps to isolate the DC bias from the RF signal paths. This approach not only reduces the potential for signal distortion but also limits the thermal and electrical stress on individual components, thereby improving the overall system lifespan.

From a compliance and safety perspective, the antenna's radiation characteristics were evaluated in the context of electromagnetic exposure. Although the design is not intended for wearable use, simulated operation at typical user distances suggests low risk of near-field exposure. The antenna's directional radiation profile inherently reduces backward radiation toward users, aligning with international guidelines such as FCC and ICNIRP standards. Combined with the robust mechanical configuration, these factors support the antenna's suitability for integration into modern wireless systems requiring reliable, multi-band performance with safe operation parameters.

V. Conclusions

This paper presents a frequency and pattern-reconfigurable rectangular microstrip patch antenna using a single PIN diode as a switching element. The antenna exhibits two operational modes, controlled by the diode's ON and OFF states, achieving multi-band functionality with resonances at 3.10 GHz, 5.00 GHz, 5.55 GHz, 7.15 GHz, and 7.75 GHz. Pattern reconfiguration is observed at 7.15 GHz and 7.75 GHz, demonstrating versatility for advanced wireless systems. A key advantage of this design is the incorporation of only one PIN diode, which simplifies the biasing circuitry and minimizes unwanted distortion that typically arises from the use of multiple switching devices. Additionally, the placement of the biasing components away from the radiating section helps maintain stable radiation patterns. Fabricated on a low-cost FR4 substrate, the antenna shows strong agreement between simulation and experimental results, validating its practical viability. Furthermore, reliability assessments based on environmental stress tolerance and safety evaluations in terms of electromagnetic exposure confirm the antenna's robustness and compliance with SAR regulations. These findings enhance the antenna's suitability for long-term deployment in modern wireless platforms. Overall, the proposed structure offers a compact, cost-effective, and efficient solution for multi-band and reconfigurable applications, with future scope including size reduction, improved material durability, and deeper system-level integration.

References

- [1] A. K. Singh, M. P. Abegaonkar, S. K. Koul. (2018). Miniaturized multiband microstrip patch antenna using metamaterial loading for wireless application, *Progress In Electromagnetics Research C*, 83:71–82.
- [2] S. Radavaram, M. Pour. (2018). Wideband radiation reconfigurable microstrip patch antenna loaded with two inverted U-slots, *IEEE Transactions on Antennas and Propagation*, 67(3):1501–1508.

- [3] T. Sabapathy, M. A. Bashah, M. Jusoh, P. J. Soh, M. R. Kamarudin. (2016). Frequency reconfigurable rectangular antenna with T-slotted feed line. In *2016 International Conference on Radar, Antenna, Microwave, Electronics, and Telecommunications (ICRAMET)*, 81–84.
- [4] Y. P. Selvam, et al. (2017). A low-profile frequency-and pattern-reconfigurable antenna. *IEEE Antennas and Wireless Propagation Letters*, 16:3047–3050.
- [5] Ali, S. Pathan, R. C. Biradar. (2016). A novel frequency reconfigurable rectangular step slotted antenna for WLAN/ITU. *International Conference on Advanced Networks and Telecommunications Systems (ANTS) IEEE*, 1–6.
- [6] D. S. Yeole, U. P. Khot. (2016). Reconfigurable multiband microstrip patch antenna design for wireless communication applications. *International Conference on Recent Trends in Electronics, Information & Communication Technology (RTEICT) IEEE*, 633–636.
- [7] A. Mansoul, M. L. Seddiki. (2018). Multiband reconfigurable Bowtie slot antenna using switchable slot extensions for WiFi, WiMAX, and WLAN applications. *Microwave and Optical Technology Letters*, 60(2):413–418.
- [8] W. Lee, H. Kim, Y. J. Yoon. (2008). A frequency reconfigurable bow-tie slot antenna with wide bandwidth. *Microwave and Optical Technology Letters*, 50(2):404–406.
- [9] N. Nguyen-Trong, L. Hall, C. Fumeaux. (2017). A dual-band dual-pattern frequency-reconfigurable antenna. *Microwave and Optical Technology Letters*, 59(11):2710–2715.
- [10] Y. P. Selvam, et al. (2017). Novel frequency-and pattern-reconfigurable rhombic patch antenna with switchable polarization. *IEEE Antennas and Wireless Propagation Letters*, 16:1639–1642.
- [11] S. Chagharvand, et al. (2015). Reconfigurable multiband tapered slot antenna. *Microwave and Optical Technology Letters*, 57(9):2182–2186.
- [12] H. A. Majid, et al. (2014). Frequency and pattern reconfigurable slot antenna. *IEEE Transactions on Antennas and Propagation*, 62(10):5339–5343.
- [13] S. J. Ha, et al. (2012). Reconfigurable beam-steering antenna using dipole and loop combined structure for wearable applications. *ETRI Journal*, 34(1):1–8.
- [14] M. Mani, et al. (2020). Frequency reconfigurable stepped impedance dipole antenna for wireless applications. *AEU-International Journal of Electronics and Communications*, 115:153029.
- [15] D. K. Borakhade, S. B. Pokle. (2015). Pentagon slot resonator frequency reconfigurable antenna for wideband reconfiguration. *AEU-International Journal of Electronics and Communications*, 69(10):1562–1568.
- [16] N. K. Sahu, A. K. Sharma. (2017). An investigation of pattern and frequency reconfigurable microstrip slot antenna using PIN diodes. In *2017 Progress In Electromagnetics Research Symposium-Spring (PIERS)*, IEEE, 971–976.
- [17] Chilukuri, S., Rangaiah, Y. P., Lokam, A., & Dahal, K. (2018). A multi-band frequency and pattern reconfigurable antenna for Wi-Fi/WiMAX and WLAN applications: frequency and pattern reconfigurable antenna. *9th International Conference on Mechanical and Aerospace Engineering (ICMAE) IEEE*, 208–212.
- [18] N. Nguyen-Trong, L. Hall, C. Fumeaux. (2016). A frequency-and pattern-reconfigurable center-shortened microstrip antenna. *IEEE Antennas and Wireless Propagation Letters*, 15:1955–1958.
- [19] A. M. Yadav, C. J. Panagamuwa, R. D. Seager. (2011). Investigation of a plug hole shaped frequency and pattern reconfigurable antenna using photo-conductive microwave switches. *41st European Microwave Conference, IEEE*, 878–881.
- [20] D. N. Elsheakh. (2019). Frequency reconfigurable and radiation pattern steering of monopole antenna based on graphene pads. *APS Topical Conference on Antennas and Propagation in Wireless Communications (APWC) IEEE*, 436–440.
- [21] A. Ghaffar, X. J. Li, N. Hussain, W. A. Awan. (2020). Flexible frequency and radiation pattern reconfigurable antenna for multi-band applications. *4th Australian microwave symposium (AMS) IEEE*, 1–2